Supporting information

An Experimental and Theoretical Mechanistic Study of Biexciton Quantum Yield Enhancement in Single Quantum Dots near Gold Nanoparticles

Swayandipta Dey[†], *Yadong Zhou*[‡], *Xiangdong Tian*[†], *Julie Jenkins*[†], *Ou Chen*[§], *Shengli Zou*[‡], *Jing Zhao*[†#]*

[†]Department of Chemistry, University of Connecticut, 55 North Eagleville Rd, Storrs, CT, 06269-3060, USA

[‡]Department of Chemistry, University of Central Florida, 4111 Libra Drive, Orlando, Florida 32816-2366, USA

[§] Department of Chemistry, Massachusetts Institute of Technology, 77 Massachusetts Avenue, Cambridge, MA 02139, USA

[#]Institute of Materials Science, University of Connecticut, Storrs, CT, 06269-3136, USA

* Address Correspondence to: jing.zhao@uconn.edu (J. Z.)

1. Calculations of average photons absorbed, <N>

The absorption cross-section $C_{abs}(\omega)$ of CdSe/CdS quantum dots(QDs) is calculated using the equations developed earlier by Leatherdale et al[1]:

$$C_{abs}(\omega) = \frac{\omega}{m_3 c}|f(\omega)^2|2n_1k_1\frac{4}{3}\pi R^3 = \frac{1}{\lambda m_3}|f(\omega)^2|2n_1k_1\frac{4}{3}\pi R^3 = \varsigma R^3$$

$$f(\omega) = \frac{3m_3^2}{m_1^2+2m_3^2}$$

where n_1, k_1 are the real and imaginary part of the bulk absorption coefficient, R is the radius of the QD and m_3, is the refractive index(R.I.) of the medium (Toluene, RI = 1.496 at 20 ºC).The parameter f is the local field factor where m_1=n_1 + ik_1 is the complex R.I. of the QD.

For the core/shell QDs, the absorption cross-section is averaged over the QD volume as reported earlier[2, 3]:

$$C_{abs}(\omega) = \varsigma_\omega^{core}R_c^3 + \varsigma_\omega^{shell}[(R_C+T_S)^3 - R_C^3] = \varsigma_\omega^{shell}[(R_C+T_S)^3] + (\varsigma_\omega^{core} - \varsigma_\omega^{shell})R_c^3$$

where R_C = radius of the CdSe core, R_S = thickness of the CdS shell.

For our CdSe/CdS QDs, R_C = 1.5nm and T_S = 3nm and the refractive indices of CdSe and CdS are obtained from Palik et al[4].

Under 532 nm excitation, ς_ω^{core} = 4.3141 × 10^4 cm^{-1} and ς_ω^{shell} = 2.6326 × 10^4 cm^{-1}.

Using the above equations for the absorption cross-section of the CdSe/CdS QDs, the calculated $C_{abs}(\omega)$ at 532nm = 2.4557 ×10^{-15} cm^2.

For the single QD measurements, we assume the spot size to be diffraction limited.

Therefore, the spot size = $\frac{1.22 \times \lambda}{NA}$ = 7.823 × 10^{-9} cm^2 (where NA = 1.30 for the objective used).

The excitation rate = $\frac{C_{abs} \times excitation\ power}{E_{photon} \times spot\ size}$ = 4.207 × 10^4 sec^{-1} where the excitation power we used for our study is 50nW.

The excitation power density is = $\frac{50 \times 10^{-9}\ W}{7.823 \times 10^{-9}\ cm^2} = 6.4\ W/cm^2$

And, the average photon absorbed per exciton lifecycle,

$\langle N \rangle$ = excitation rate × PL lifetime (τ) = 4.207×10^{4} sec^{-1} × 38×10^{-9} sec ≈ 0.0015

The ensemble PL lifetime (τ) of the CdSe/CdS QDs on the glass substrate was obtained by fitting the decay in Figure 5 (black curve) with a single exponential decay function.

2. SEM, TEM and extinction of Au@SiO_2-5 nm substrate

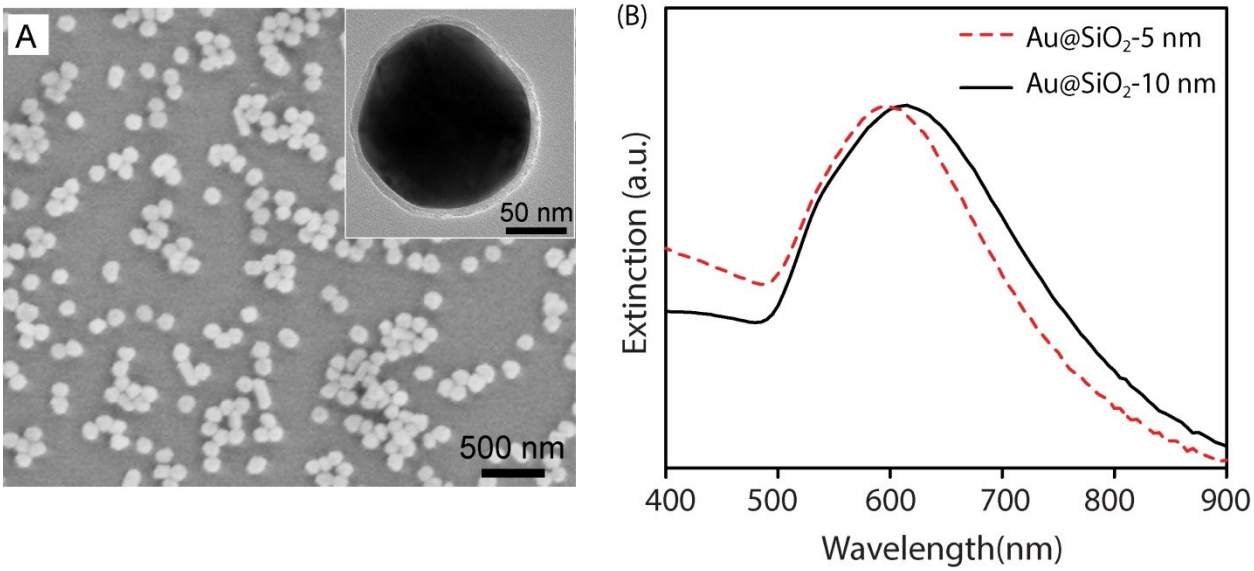

Figures S1. (A) SEM images of Au@SiO_2 NPs substrates with silica shell thickness of 5±1 nm. The insets in the figures are the corresponding high resolution TEM images of the Au@SiO_2 NPs. (B) Extinction spectra of Au@SiO_2-5nm(red) and Au@SiO_2-10nm(black) nanoparticles in water.

The LSPR of Au@SiO_2-5 nm peaks at 597 nm and Au@SiO_2-10 nm peaks at 612 nm. The LSPR of Au@SiO_2-10 nm is red-shifted (15 nm) from that of Au@SiO_2-5 nm, because the local dielectric constant of the Au NP is increased when the silica shell is thicker.

3. Blinking traces and $g^2(\tau)$ data and "on"/ "off" times distribution of of a QD on Au@SiO_2-5 nm substrate

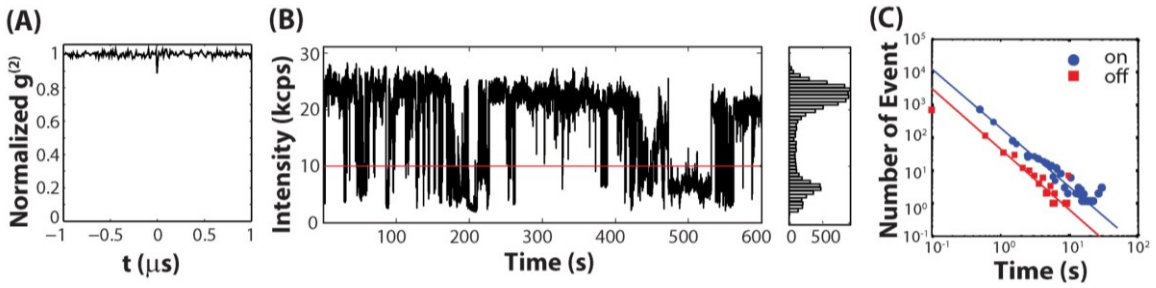

Figure S2.Representative $g^{(2)}$ measurements (A) blinking traces (B) and log-log plots of the "on","off" time statistics of QDs (C) on Au@SiO_2-5nm. Histograms indicating the distribution of intensities observed in the time trace.

4. Blinking traces and $g^2(\tau)$ data of the representative single QDs on glass substrate

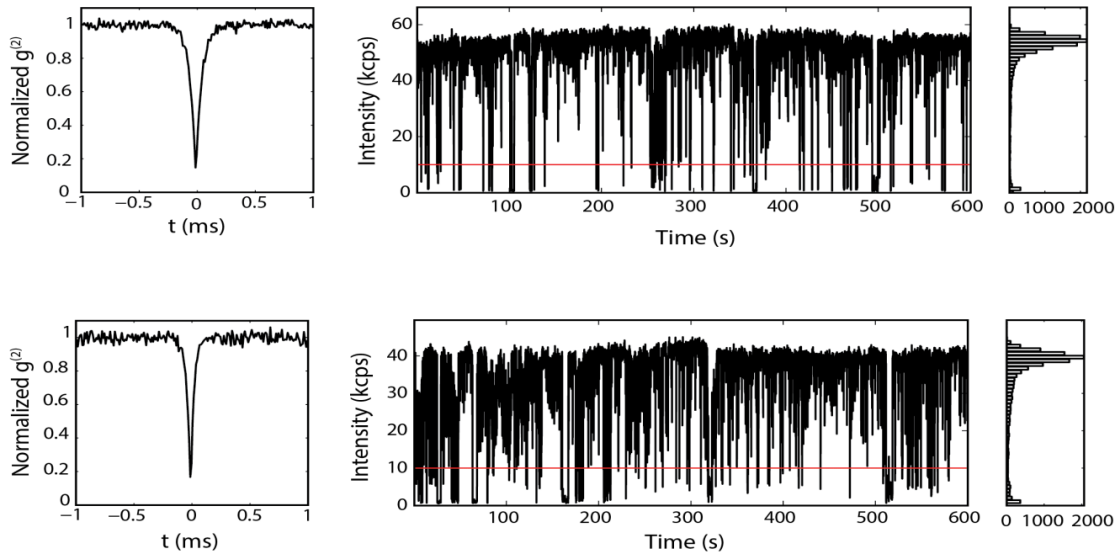

Figure S3. Representative $g^{(2)}$ measurements and corresponding blinking traces of single QDs on glass.

5. Blinking traces and $g^2(\tau)$ data of the representative single QDs on Au@SiO_2-5nm substrate

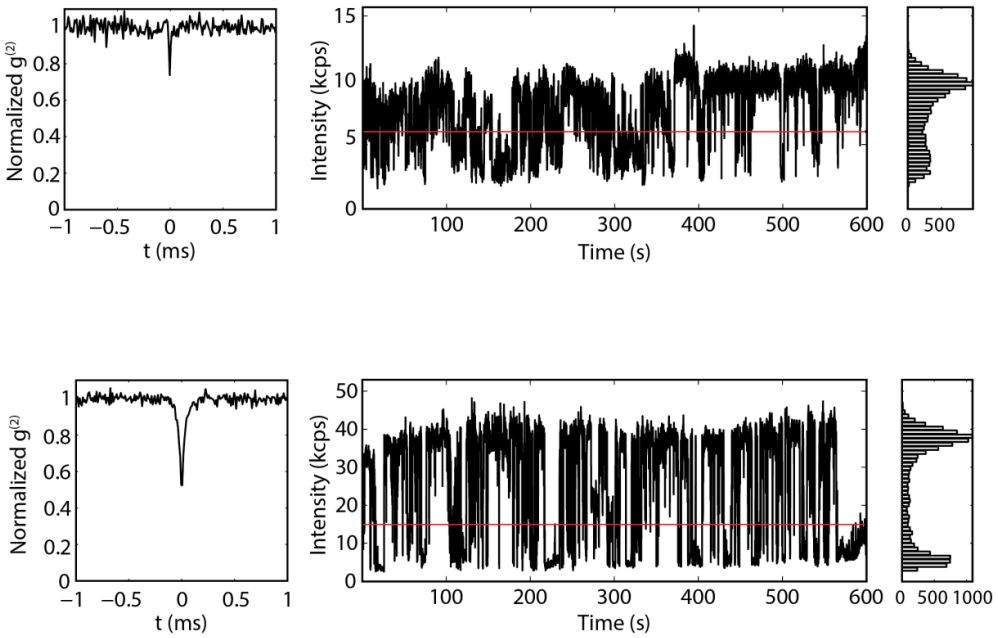

Figure S4. Representative $g^{(2)}$ measurements and corresponding blinking traces of single QDs on Au@SiO_2-5nm substrate.

6. Blinking traces and $g^2(\tau)$ data of the representative single QDs on Au@SiO_2-10nm substrate

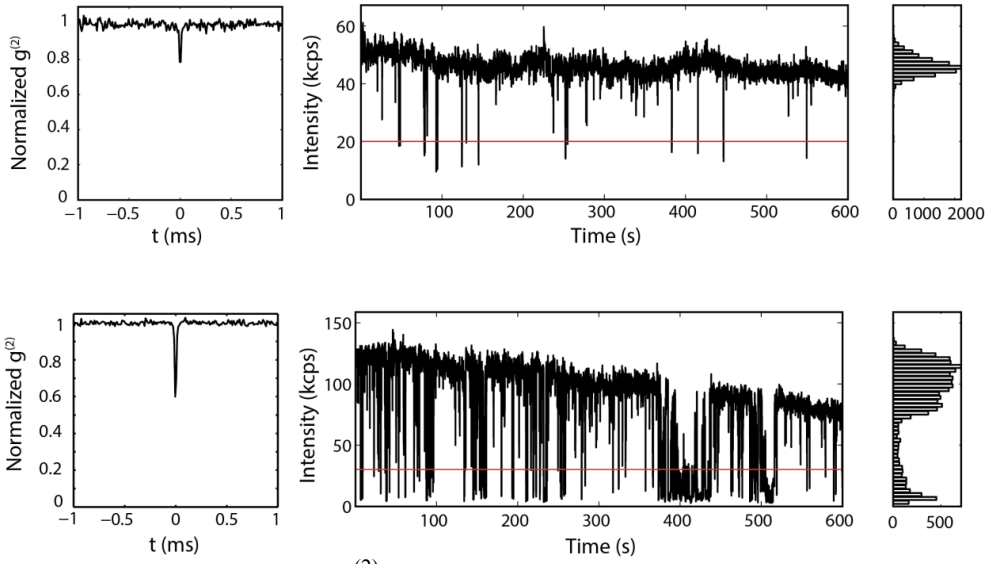

Figure S5. Representative $g^{(2)}$ measurements and corresponding blinking traces of single QDs on Au@SiO_2-10nm substrate.

7. Blinking Statistics

The PL blinking traces and intensity histograms of single QDs (shown in Figure 3B, 3E and S1-B) clearly demonstrate that the QDs all exhibit a two-state blinking with well-defined "on" and "off" states whether they are on glass or Au@SiO_2 NPs. The red lines in these denote the threshold between the "on" and "off" events. For quantitative analysis, the corresponding statistics of "on" and "off" times are calculated from the blinking traces and plotted in Figure 3B, 3E and S1-B. The lines in the plots are the power-law fit for the "on"/ "off" statistics. All the distributions for "on" and "off" event durations fit well to power-law distribution where $Number\ of\ events \propto {t_{on/off}}^{-\alpha_{on/off}}$. In the power-law function, $t_{on/off}$ represents the time intervals that a QD stays in an "on" or "off" state, and $\alpha_{on/off}$ represents the power-law exponents. For the CdSe/CdS QDs on glass, α_{on}= 0.85 and α_{off} = 1.5. The small α_{on} for the QDs is consistent with previous study and showing that the QDs have long "on" times. When the QDs were adsorbed on Au@SiO_2 NP substrates, the "on"/"off" statistics still follows power-law distribution but values of $\alpha_{on/off}$ have changed. And more interestingly, the values of α_{on} and α_{off} are similar for the QDs on Au@SiO_2 NP. The calculated $\alpha_{on/off}$for QDs on Au@SiO_2 NP with ~ 5 nm silica shell are α_{on}= 1.8 and α_{off} = 1.85; and for QDs on Au@SiO_2 NP with ~ 10 nm silica shell, both α_{on} and α_{off} are 1.5. The dwell times for the "on"/"off" events of the single QDs are altered by the presence of the Au NPs, especially the "on" events. The results indicate the plasmonic structures may be used to modify the photo darkening process in QD films, important for their application in light emitting devices.

8. $g^2(\tau)$ dip value distribution for QDs on Au@SiO_2-5nm substrate

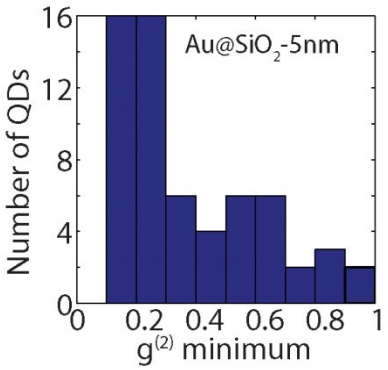

Figure S6. Histograms of the minimum $g^{(2)}$ data of single QDs on Au@SiO_2-5nm.

The difference in the $g^2(\tau)$ values distribution of QDs on Au@SiO_2 NP substrates may be related to how the Au@SiO_2 NPs were distributed on glass. We reexamined the SEM images of the Au@SiO_2-5 nm (Figure S2-A) and Au@SiO_2-10 nm (Figure 1C) substrates. It is clear from the SEM images of the Au@SiO_2-5 nm and Au@SiO_2-10 nm substrates that the packing density of the Au@SiO_2 NPs is different on those two substrates. The Au@SiO_2-5 nm substrate has much more void space without the NPs compared to the Au@ SiO_2-10 nm substrate. A quantitative analysis revealed the packing density of the NPs on the Au@SiO_2-5 nm substrate is 60% lower than that of the Au@ SiO_2-10 nm substrate. Since the QDs were randomly spin-coated on the substrates, there is a much higher chance for the QDs to fall on empty glass than on the Au@ SiO_2-5 nm substrate. Since plasmonic effect is near-field in nature and decays fast from the metal surface, the X and BX emission of the QDs with a large distance from the NPs is much less affected than the QDs close to or on the NPs. The QDs with $g^2(\tau)$ dip values of 0.1-0.2 are likely to be situated far from the NPs thus behave like the QDs on bare glass. The two population of QDs lead to the broad distribution of $g^2(\tau)$ dip values. We also show in the calculations that not only the distance between the QD and NP, but also the relative position and the orientation of the QD/NP complex determines the exciton-plasmon coupling strength.

9. Ensemble PL decay

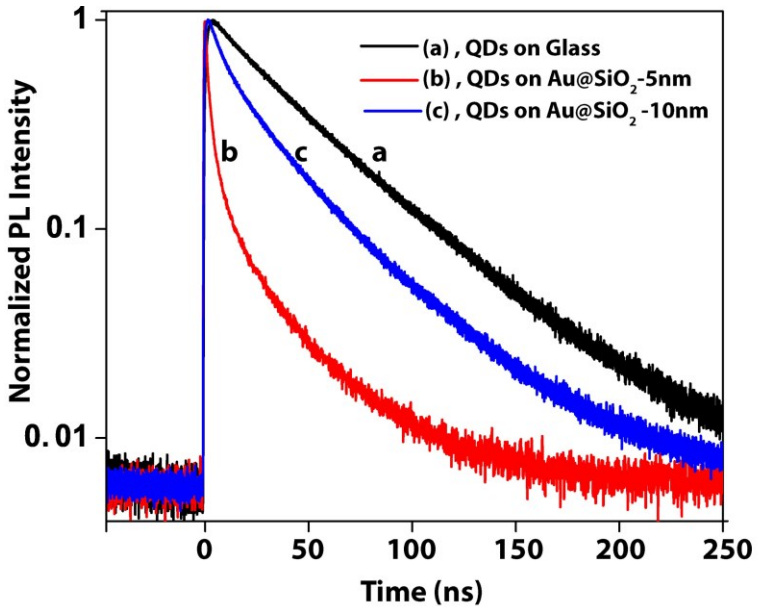

Figure S7. Ensemble PL decay CdSe/CdS QDs on different substrates (a) on glass (b) on Au@SiO_2-5nm (c) on Au@SiO_2-10nm.

The PL decay of the QDs on glass (Figure S7, a-black curve) fits well with a bi-exponential decay function of $y = 2.23e^{-t/25.4} + 1.83e^{-t/53.2}$. For the QDs on Au@$SiO_2$-5 nm, the PL decay ((Figure S7, b-red line) fits with $y = 5.81 \times 10^4 e^{-t/4.03} + 0.69e^{-t/28.8}$. For the QDs on Au@$SiO_2$-10 nm, the PL decay (Figure S7, c-blue line) fits with $y = 2.49 \times 10^2 e^{-t/8.28} + 1.57e^{-t/45.5}$. The fittings show that for the QDs on MNP substrate, the decay process was dominated by a fast decay at shorter times and there was also a much slower decay at longer times.

10. Calculations of distance-dependent BX QY/X QY

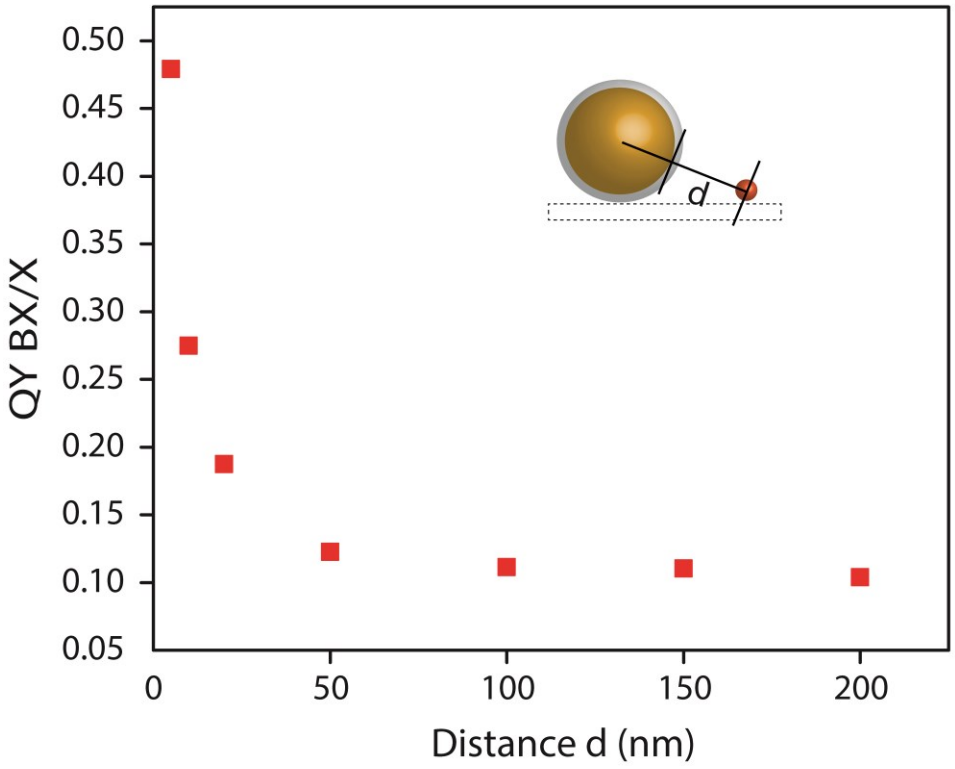

Figure S8. Calculated interparticle distance dependent ratio of BX QY to X QY of a single QD near an Au@SiO_2 nanoparticle. The scheme shows how distance d is defined in the calculations.

Table S1. Theoretical results of the averaged X, BX intensity, lifetime and quantum yield of a QD on a Au@SiO_2 monomer with varying incident polarization angle

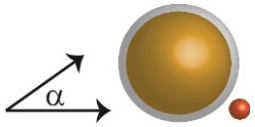

	Silica shell thickness = 5 nm					Average
α	**0**	**30**	**45**	**60**	**90**	
$\|E\|^2$	2.01	1.87	1.73	1.59	1.45	1.73
Rel. X PL Intensity	0.75	0.64	0.52	0.38	0.24	0.50
Rel. BX PL Intensity	7.83	5.85	4.11	2.60	1.31	4.34
Rel. X PL lifetime	0.10	0.11	0.12	0.15	0.17	0.13
Rel. BX PL lifetime	0.51	0.54	0.58	0.62	0.67	0.58
X PL QY	0.35	0.32	0.28	0.23	0.15	0.27
BX PL QY	0.19	0.17	0.14	0.10	0.06	0.13
Ratio (BX QY/ X QY)	0.55	0.52	0.48	0.45	0.40	0.48

	Silica shell thickness = 10 nm					Average
α	**0**	**30**	**45**	**60**	**90**	
$\|E\|^2$	1.74	1.68	1.63	1.57	1.52	1.63
Rel. X PL Intensity	1.02	0.93	0.83	0.70	0.53	0.80
Rel. BX PL Intensity	5.82	4.68	3.58	2.52	1.49	3.62
Rel. X PL lifetime	0.22	0.26	0.30	0.37	0.48	0.33
Rel. BX PL lifetime	0.73	0.77	0.81	0.85	0.90	0.81
X PL QY	0.55	0.52	0.48	0.43	0.33	0.47
BX PL QY	0.19	0.16	0.14	0.10	0.07	0.13
Ratio (BX QY/ X QY)	0.35	0.31	0.28	0.24	0.20	0.27

Table S2. Theoretical results of the averaged X, BX intensity, lifetime and quantum yield of a QD on a Au@SiO_2 dimer with varying angle of QD relative to the Au-Au NP center axis. The incident polarization is either parallel or perpendicular to the Au-Au NP center axis.

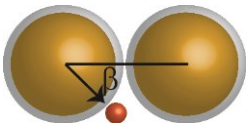

	Silica shell thickness = 5 nm									Ave-
β	**0**	**30**	**45**	**60**	**90**	**120**	**135**	**150**	**180**	**rage**
$\|E\|^2$ (||)	1.69	1.64	1.60	1.55	1.76	1.93	2.07	2.21	1.78	1.96
(⊥)	1.79	2.00	2.20	2.39	2.54	2.34	2.17	2.02	1.88	
Rel. X PL Int (||)	0.86	0.77	0.64	0.45	0.25	0.54	0.71	0.83	0.94	0.70
(⊥)	0.38	0.65	0.86	1.04	1.13	0.88	0.72	0.57	0.43	
Rel. BX PL Int (||)	7.16	5.63	4.00	2.35	1.07	3.25	5.15	7.00	9.00	5.64
(⊥)	1.93	4.37	7.34	10.6	12.8	8.16	5.62	3.77	2.33	
Rel. X PL lifetime (||)	0.11	0.14	0.17	0.23	0.30	0.22	0.19	0.16	0.15	0.20
(⊥)	0.29	0.22	0.18	0.15	0.14	0.17	0.20	0.24	0.28	
Rel. BX PL lifetime (||)	0.54	0.59	0.66	0.73	0.79	0.72	0.67	0.64	0.61	0.68
(⊥)	0.79	0.72	0.66	0.62	0.59	0.65	0.69	0.74	0.78	
X PL QY (||)	0.48	0.45	0.38	0.28	0.15	0.29	0.35	0.38	0.40	0.36
(⊥)	0.21	0.32	0.39	0.44	0.44	0.38	0.33	0.28	0.23	
BX PL QY (||)	0.25	0.21	0.16	0.10	0.05	0.10	0.14	0.16	0.18	0.14
(⊥)	0.06	0.11	0.15	0.18	0.20	0.15	.0.12	0.09	0.07	
Ratio(BXQY/XQY) (||)	0.52	0.47	0.41	0.35	0.29	0.36	0.40	0.43	0.45	0.39
(⊥)	0.30	0.36	0.41	0.45	0.47	0.42	0.38	0.34	0.30	
	Silica shell thickness = 10 nm									**Ave-**
β	**0**	**30**	**45**	**60**	**90**	**120**	**135**	**150**	**180**	**rage**
$\|E\|^2$ (||)	1.54	1.54	2.15	1.56	1.63	1.80	1.89	1.98	2.05	1.90
(⊥)	2.00	2.08	2.15	2.22	2.23	2.10	2.03	1.96	1.90	
Rel. X PL Int (||)	0.97	0.92	0.84	0.72	0.54	0.83	0.99	1.10	1.20	0.96
(⊥)	0.68	0.97	1.15	1.28	1.31	1.13	1.00	0.88	0.74	
Rel. BX PL Int (||)	5.17	4.33	3.39	2.36	1.45	3.15	4.56	5.92	7.31	4.67
(⊥)	2.12	4.15	6.20	8.11	8.99	6.26	4.71	3.46	2.37	
Rel. X PL lifetime (||)	0.21	0.26	0.32	0.43	0.58	0.43	0.35	0.30	0.27	0.38
(⊥)	0.61	0.44	0.34	0.28	0.26	0.32	0.38	0.45	0.56	
Rel. BX PL lifetime (||)	0.71	0.76	0.81	0.87	0.93	0.87	0.83	0.80	0.77	0.83
(⊥)	0.93	0.87	0.82	0.78	0.76	0.81	0.84	0.88	0.92	
X PL QY (||)	0.60	0.57	0.36	0.44	0.31	0.44	0.49	0.53	0.55	0.48
(⊥)	0.32	0.45	0.50	0.54	0.56	0.50	0.47	0.43	0.37	
BX PL QY (||)	0.22	0.18	0.14	0.10	0.05	0.10	0.13	0.15	0.17	0.13
(⊥)	0.05	0.10	0.13	0.17	0.18	0.14	0.11	0.09	0.06	
Ratio(BXQY/XQY) (||)	0.37	0.32	0.27	0.22	0.17	0.22	0.26	0.29	0.31	0.25
(⊥)	0.16	0.22	0.26	0.30	0.32	0.28	0.24	0.21	0.18	

References:

1) Leatherdale, C. A.; Woo, W. K.; Mikulec, F. V.; and Bawendi, M. G., *J. Phys. Chem. B*, **2002**, *106*, 7619.
2) Park, Y.-S.; Klimov, V. I. and Htoon, H, *Phys.Rev.Lett*., **2011**, *106*, 18, 187401.
3) Zhao, J; Chen, O; Strasfeld, D. B and Bawendi,M.G., *Nano Lett*., **2012**, *12*, 4477.
4) *Handbook of Optical Constants II*, Palik, E.D., Academic Press, Boston, **1991**.
5) Chen, O.; Zhao, J.; Chauhan, V. P.; Cui, J.; Wong, C.; Harris, D. K.; Wei, H.; Han, H.-S.; Fukumura, D.; Jain, R. K.; Bawendi, M. G. Nat. Mater. 2013, 12, 445-451.